Neuroscience 297 (2015) 127–136

REDUCTIONS OF DOCOSAHEXAENOIC ACID-CONTAINING PHOSPHATIDYLCHOLINE LEVELS IN THE ANTERIOR HORN OF AN ALS MOUSE MODEL

H. ARIMA,[a,b] T. OMURA,[a] T. HAYASAKA,[b,f] N. MASAKI,[b] M. HANADA,[a] D. XU,[a] T. BANNO,[a] K. KOBAYASHI,[c] H. TAKEUCHI,[d] K. KADOMATSU,[e] Y. MATSUYAMA[a] AND M. SETOU[b,g,h]*

[a] *Department of Orthopedic Surgery, Hamamatsu University School of Medicine, Japan, 1-20-1 Handayama, Higashi-ku, Hamamatsu, Shizuoka 431-3192, Japan*

[b] *Department of Cell Biology and Anatomy, Hamamatsu University School of Medicine, Japan, 1-20-1 Handayama, Higashi-ku, Hamamatsu, Shizuoka 431-3192, Japan*

[c] *Department of Orthopedics, Nagoya University Graduate School of Medicine, Japan, 65 Tsurumai-cho, Showa-ku, Nagoya, Aichi 466-8550, Japan*

[d] *Department of Neuroimmunology, Research Institute of Environmental Medicine, Nagoya University, Japan, Furo-cho, Chikusa-ku, Nagoya, Aichi 464-8601, Japan*

[e] *Department of Biochemistry, Nagoya University Graduate School of Medicine, Japan, 65 Tsurumai-cho, Showa-ku, Nagoya, Aichi 466-8550, Japan*

[f] *Faculty of Health Science, Hokkaido University Graduate School of Medicine, Japan, Kita 12, Nishi 5, Kita-ku, Sapporo, Hokkaido 060-0812, Japan*

[g] *Department of Anatomy, The University of Hong Kong, Pok Fu Lam, 999077, Hong Kong*

[h] *JST, ERATO, Sato project, Tokyo 160-8582, Japan*

Abstract—In this study, we analyzed the spatiotemporal alterations of phospholipid composition in the spinal cord of an amyotrophic lateral sclerosis (ALS) mouse model (G93A-mutated human superoxide dismutase 1 transgenic mice [SOD1^{G93A} mice]) using imaging mass spectrometry (IMS), a powerful method to visualize spatial distributions of various types of molecules *in situ*. Using this technique, we deciphered the phospholipid distribution in the pre-symptomatic stage, early stage after disease onset, and terminal stages of disease in female SOD1^{G93A} mouse spinal cords. These experiments revealed a significant decrease in levels of docosahexaenoic acid (DHA)-containing phosphatidylcholines (PCs), such as PC (diacyl-16:0/22:6), PC (diacyl-18:0/22:6), and PC (diacyl-18:1/22:6) in the L5 anterior horns of terminal stage (22-week-old) SOD1^{G93A} mice. The reduction in PC (diacyl-16:0/22:6) level could be reflecting the loss of motor neurons themselves in the anterior horn of the spinal cord in ALS model mice. In contrast, other PCs, such as PC (diacyl-16:0/16:0), were observed specifically in the L5 dorsal horn gray matter, and their levels did not vary between ALS model mice and controls. Thus, our study showed a significant decrease in DHA-containing PCs, but not other PCs, in the terminal stage of ALS in model mice, which is likely to be a reflection of neuronal loss in the anterior horns of the spinal cords. Given its enrichment in dorsal sensory regions, the preservation of PC (diacyl-16:0/16:0) may be the result of spinal sensory neurons being unaffected in ALS. Taken together, these findings suggest that ALS spinal cords show significant alterations in PC metabolism only at the terminal stage of the disease, and that these changes are confined to specific anatomical regions and cell types.

Key words: ALS, imaging mass spectrometry, phosphatidylcholine, DHA, anterior horn, neuronal loss.

INTRODUCTION

Amyotrophic lateral sclerosis (ALS) is a progressive, life-threatening neurodegenerative disease caused by the degeneration of upper and lower motor neurons in the cortex, brain stem, and spinal cord (Rosen et al., 1993; Bruijn et al., 1998; Clement et al., 2003). Approximately 90% of cases of ALS appear to be sporadic without a family history of the disease. The remaining 10% of patients are diagnosed with familial ALS (fALS), and approximately 20% of these familial cases are caused by dominant mutations in Cu/Zn superoxide dismutase 1 (SOD1) (Bruijn et al., 1998; Clement et al., 2003; Di Giorgio et al., 2007). A widely used transgenic mouse model of fALS (SOD1^{G93A} mice) has been developed through the insertion of a G93A-mutated human SOD1 transgene into the murine genome (Gurney et al., 1994; Bendotti and Carri, 2004; Takeuchi et al., 2011). SOD1^{G93A} mice show severe atrophy in the anterior horns of the spinal cord characterized by marked neuronal loss and activation of microglia and astrocytes, as is observed in patients with ALS (Bendotti and Carri, 2004; Takeuchi et al., 2011; Acquadro et al., 2014). However, the biochemical and molecular pathogenesis of ALS remains

*Correspondence to: M. Setou, Department of Cell Biology and Anatomy, Hamamatsu University School of Medicine, Japan, 1-20-1 Handayama, Higashi-ku, Hamamatsu, Shizuoka 431-3192, Japan. Tel: +81-53-434-5282; fax: +81-53-435-2468.
E-mail address: setou@hama-med.ac.jp (M. Setou).

Abbreviations: ALS, Amyotrophic lateral sclerosis; CMC, carboxymethyl cellulose; DHA, docosahexaenoic acid; DHB, dihydroxybenzoic acid; EPA, eicosapentaenoic acid; FA, fatty acid; IMS, imaging mass spectrometry; MALDI, matrix-assisted laser desorption/ionization; PC, phosphatidylcholine; PUFA, polyunsaturated fatty acids; SOD, superoxide dismutase; TOF, time-of-flight.

http://dx.doi.org/10.1016/j.neuroscience.2015.03.060

unclear, and effective therapeutic approaches have not yet been established for treating ALS (Hirano et al., 2013).

The most abundant biomolecules in the central nerve system, including the spinal cord, are lipids, which function to facilitate vesicle fusion, regulate ion flux, and create specialized microenvironments that promote cellular communication (Piomelli et al., 2007). Recently, imaging mass spectrometry (IMS) has emerged as a promising new technology that enables simultaneous imaging of many types of biomolecules including lipids (Hayasaka et al., 2008; Sugiura and Setou, 2010). This technique thereby advances the ability to investigate alterations in the distribution of the molecular components of specific areas of the central nervous system in diseases states, thus providing further insights into new therapeutic targets for human pathologies (Wisztorski et al., 2008; Acquadro et al., 2014). Using this technique, we recently observed changes in lipid metabolism in the spine following spinal cord injury (Hanada et al., 2012; Arima et al., 2014). In addition, matrix-assisted laser desorption/ionization (MALDI)-IMS analysis of brain tissue slices harvested from the central nervous system of disease model organisms is emerging as a powerful new means to the study neurodegenerative disease (Yuki et al., 2014). However, comprehensive studies of lipid molecules in neurodegenerative disease states using MALDI-MS are limited.

To date, two published studies utilized MALDI imaging to study molecular properties of ALS in either patient-derived specimens or animal models. An analysis of human post-mortem spinal cord samples indicated that two protein species, including a C-terminally truncated form of ubiquitin, were decreased in ALS (Hanrieder et al., 2013). The other study was carried out using $SOD1^{G93A}$ mice and found that human $SOD1^{G93A}$ protein was accumulated in the facial and trigeminal nuclei of these mice (Acquadro et al., 2014). As is the case with the majority of research into the neurobiological mechanisms of ALS, both studies focused mainly on protein alterations in the brain and spinal cord.

However, an increasing number of reports demonstrate that there are important neurobiological roles for neural lipids in health and disease (Piomelli et al., 2007). In this study, we set out to characterize alterations in the composition of phospholipids in ALS using MALDI-IMS, which is effective for detecting and visualizing phospholipid metabolism (Jackson et al., 2005, 2007; McLean et al., 2007; Hayasaka et al., 2008). The major structural phospholipids in eukaryotic membranes are the glycerophospholipids: phosphatidylcholine (PC), phosphatidylethanolamine, phosphatidylserine, phosphatidylinositol, and phosphatidic acid. PCs account for >50% of the phospholipids in most eukaryotic membranes (van Meer et al., 2008). In this study, we therefore utilized IMS to investigate the characteristics of the lipid composition in the $SOD1^{G93A}$ ALS mouse model with a focus on PC molecular species and assessed whether changes in the phospholipid composition were associated with disease progression and pathogenesis.

EXPERIMENTAL PROCEDURE

Chemicals

Methanol, potassium acetate, carboxymethyl cellulose (CMC), and ultrapure water were purchased from Wako Pure Chemical Industries (Osaka, Japan). Calibration-standard peptides and 2,5-dihydroxybenzoic acid (DHB), a MALDI matrix, were purchased from Bruker Daltonics (Fremont, CA, USA). All chemicals used in this study were of the highest purity available.

Animals and survival analysis

All the experimental procedures were approved by the Ethics Committee of the Hamamatsu University School of Medicine (Shizuoka, Japan). Transgenic mice, which carry a high copy number of a transgenic encoding a G93A mutant of human SOD1 (B6.Cg-Tg [SOD1-G93A]1Gur/J line) (Gurney et al., 1994), were purchased from the Jackson Laboratory (Bar Harbor, ME, USA). Offspring hemizygous for the mutant SOD1 transgene used in this study were produced by strict crossings of hemizygous male B6.SOD1G93A mice with wild-type C57BL/6 inbred females to maintain the mutant transgene on a C57BL/6 congenic background ($n > 10$). Isolated genomic blood DNA was used to genotype animals using a standard protocol provided by the Jackson Laboratory, as previously described (Hayworth and Gonzalez-Lima, 2009).

For image analysis, female $SOD1^{G93A}$ and non-transgenic littermate mice at the age of 5 weeks (before disease onset), 10 weeks (an early stage after disease onset), and 22 weeks (a terminal stage after onset of disease) were used ($n = 3$ for each time point). Body weight was measured once a week ($n = 4$ for each group). Food and water were provided *ad libitum*, and animals were housed three/cage in a room with a 12-h light/dark cycle. Animals with substantial motor impairment had food provided on the cage bottom and spouts of water bottles were set near the bottom of the cage. We also investigated survival time in the $SOD1^{G93A}$ group ($n = 4$ for each group). Survival time was defined as the age when the animals were unable to move right themselves within 60 s of being placed on either side of their body. At this point, the animals were deeply anesthetized with ether and then sacrificed.

Tissue preparation for IMS

Mice were anesthetized with 25 mg/kg pentobarbital sodium and killed by transcardial perfusion with cold 0.01 M phosphate-buffered saline (PBS). Mouse spinal cord specimens of approximately 2 cm in length originating around the L5 level were extracted. Segments of the spinal cord were embedded in CMC compound and sliced using a cryostat at a thickness of 10 μm (CM1950; Leica, Wetzlar, Germany) along the axial plane ($SOD1^{G93A}$ group: 5th week, $n = 3$; 10th week, $n = 3$; 22nd week, $n = 3$; and control group; 5th week, $n = 3$; 10th week, $n = 3$; 22nd week, $n = 3$). Sections were then placed directly onto glass slides

coated with indium-tin-oxide and were stored at −20 °C until matrix application and subsequent IMS.

IMS sample preparation and IMS analysis

DHB solution (50 mg/mL DHB, 20 mM potassium acetate, 70% methanol) was used as the matrix solution to detect signals of PC species. The matrix solution (approximately 500 μL) was sprayed over the tissue surface using a 0.2-mm nozzle caliber airbrush (ProCon Boy FWA Platinum; Mr. Hobby, Tokyo, Japan). Tissue sections were spray-coated with the matrix solution in order to perform extraction and co-crystallization simultaneously. The distance between the nozzle tip and tissue surface was maintained at 10 cm, and the spraying period was fixed at 20 min. IMS analyses were performed using a MALDI time-of-flight (TOF)/TOF-type instrument (ultraflex II TOF/TOF; Bruker Daltonics) equipped with a 355-mm Nd:YAG laser. Data were acquired in the positive reflectron mode under an accelerating potential of 25 kV using an external calibration method. Signals between *m/z* 400 and 1000 were collected, and raster scans of tissue surfaces were automatically obtained at a spatial resolution of 50 μm using the flexControl and flexImaging 2.0 software (Bruker Daltonics). The number of laser irradiations was 200 shots at each location, and ion image reconstruction was performed with flexImaging 2.0 software. The structures of the side chains of the glycerophospholipid species with one or two radial side chains are indicated within parentheses in the following format: head group (coupling scheme-sn-1/sn-2); e.g., PC (diacyl-16:0/18:1). Signal intensity was represented for each PC species as relative intensity to the most abundant signal, PC (diacyl-16:0/18:1) in the control group.

Immunohistochemistry

Frozen sections of the spinal cord were fixed with 2% paraformaldehyde for 15 min at room temperature. For the immunofluorescence labeling experiment, spinal cord sections were first blocked in PBS containing 1% bovine serum albumin, 2% blocking reagent (Roche, Basel, Schweiz), and 0.1% Triton X-100 for 60 min. Rabbit anti-NeuN antibody (1:500 Millipore, Billerica, MA, USA) and rabbit anti-Hb9/HLXB9 (1:250 Abcam, Cambridge, MA, USA) were incubated at 4 °C overnight. The sections were then incubated with secondary antibody conjugated with Alexa Fluor 488 donkey anti-rabbit IgG (Life Technologies, Carlsbad, CA, USA) for 1 h at room temperature. Slides were then washed and cover slips were mounted onto the slides using a solution of VECTASHIELD Mounting Medium (Funakoshi, Tokyo, Japan). All images were obtained using a scanner (NanoZoomer 2.0HT, Hamamatsu Photonics, Shizuoka, Japan) or a fluorescent microscope (AX-80, Olympus, Tokyo, Japan). We quantified the expression of Hb9, in cells with the area larger than 450 μm^2 in the anterior horn at various disease stages in $SOD1^{G93A}$ and control group (n = 3 for each group). Analysis was performed using NDP view software (Hamamatsu Photonics).

Statistical analysis

All values are expressed as mean ± SEM. Differences between groups were examined about statistical significance using the unpaired two-sample *t*-test or a one-way ANOVA test. Post-ANOVA comparisons were made using the Tukey test. $P < 0.05$ was considered as significant. The statistical analyses were performed using the Statistical Package for the Social Sciences (SPSS) software (version 21.0; SPSS, Chicago, IL, USA).

RESULTS

Characteristics of PC species in the L5 spinal cord of ALS mice in the terminal stage

To monitor disease progression, body weights of $SOD1^{G93A}$ mice were measured once a week. Weight gain diminished by 10 weeks after birth, and body weight loss began 17 weeks after birth. We began to observe significant differences in body weight between $SOD1^{G93A}$ and control mice 10 weeks after birth (Data not shown). $SOD1^{G93A}$ mice began to die at approximately 23 weeks of age, and all $SOD1^{G93A}$ mice died within 25 weeks, in accordance with previous studies (Takeuchi et al., 2011; Hirano et al., 2013; Kobayashi et al., 2013).

Given that in $SOD1^{G93A}$ mice, declines in motor function commence at around 9 weeks of age (Hirano et al., 2013), we performed MALDI-IMS analysis of the profile and distribution of PCs in spinal cord specimens obtained from mice aged five (presymptomatic stage), 10 (early stage after onset), and 22 weeks (terminal stage). MALDI-IMS analysis of the L5 spinal cord sections revealed characteristic PC distribution patterns with distinct fatty acid (FA) compositions. Specifically, we compared average mass spectra of L5 spinal cord sections in the positive ion detection mode. To evaluate the difference in composition of PC species, we obtained the average mass spectrum from the entire spinal cord at L5 which included both gray and white matter, for control (Fig. 1A) and in $SOD1^{G93A}$ mice (Fig. 1B) at the age of 22 weeks. Relative abundance was determined to the most abundant signal. We then defined signal intensity according to the relative abundance to the most abundant PC signal (diacyl-16:0/18:1) observed in the control mice. Approximately 150 mass peaks in the range of $700 < m/z < 880$ were detected. Among these peaks, 12 intense peaks were assigned as PC species based on their masses and previous reports (Sugiura et al., 2009; Hanada et al., 2012). The peaks at *m/z* 770.4, 772.4, 798.4, 820.5, 824.5, 826.5, 844.5, 846.5, 848.5, 870.6, and 872.6 were identified as PC (diacyl-16:0/16:1), PC (diacyl-16:0/16:0), PC (diacyl-16:0/18:1), PC (diacyl-16:0/20:4), PC (diacyl-18:1/18:1), PC (diacyl-18:0/18:1), PC (diacyl-16:0/22:6), PC (diacyl-18:1/20:4), PC

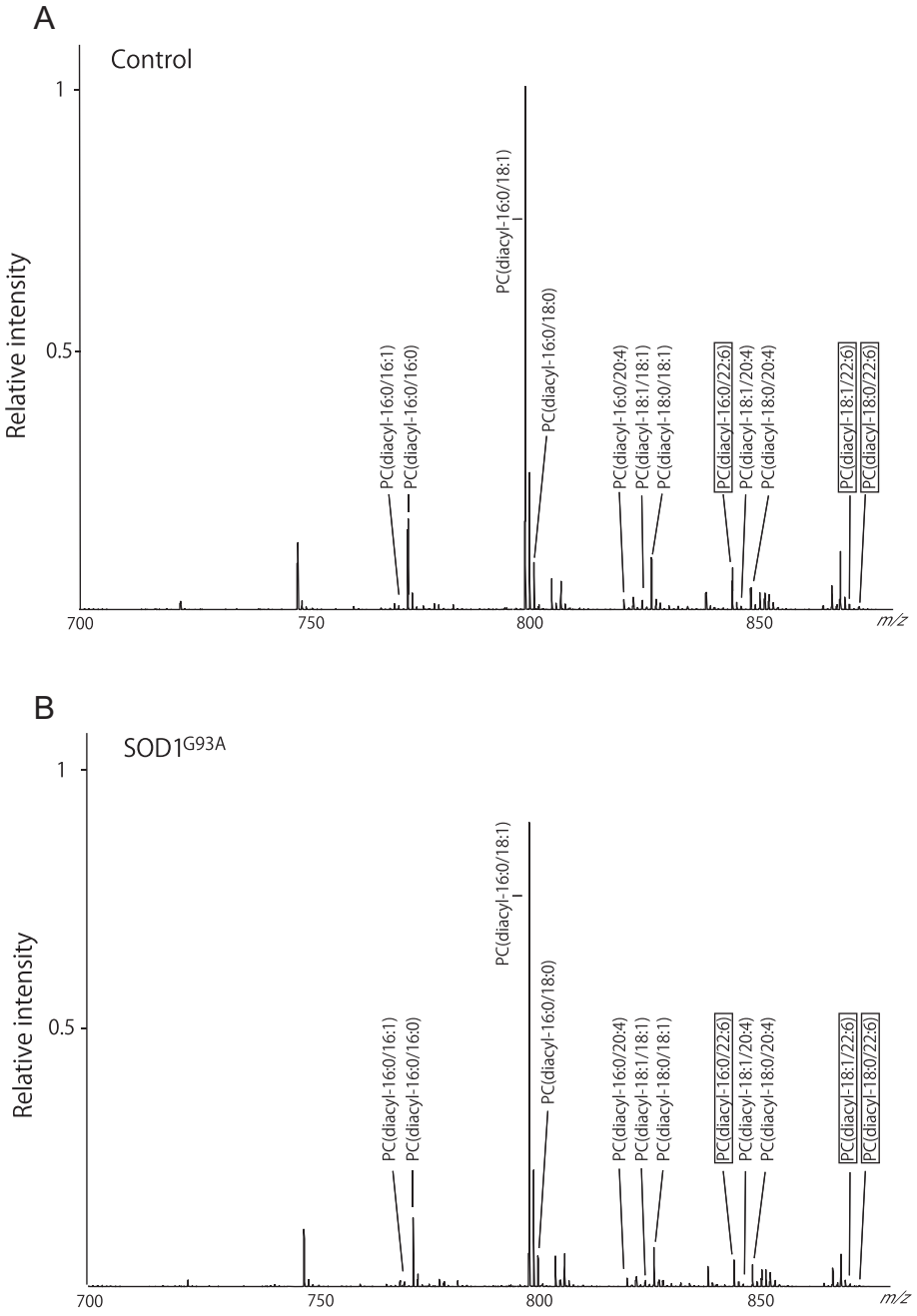

Fig. 1. Assignment of characteristic PC species at 22 weeks in control and SOD1^{G93A} mice. A representative mass spectrum was obtained using MALDI-IMS from L5 axial spinal cord sections. Signal intensity corresponds to the relative abundance to the most abundant signal for PC (diacyl-16:0/18:1) in the control group (A). We detected approximately 150 mass peaks in the *m/z* range from 700 to 880. Among these peaks, we assigned 11 intense peaks as PC species based on a database search and previous reports. The mean signal intensities of the three PCs are surrounded by squares; PC (diacyl-16:0/22:6), PC (diacyl-16:0/18:1) and PC (diacyl-16:0/20:4), were lower in the SOD1^{G93A} mouse compared to the control (A, B).

(diacyl-18:0/20:4), PC (diacyl-18:1/22:6), and PC (diacyl-18:0/22:6), respectively (Fig. 1A, B).

Visualization of PC species in L5 spinal cord of ALS mice in the terminal stage

The spectra in Fig. 1A, B represent qualitative data from the entire spinal cord section at the level of L5 obtained from 22-week-old control and SOD1^{G93A} mice. We then reconstructed 11 ion images of the major PC molecular species by using the flexImaging 2.0 software in order to analyze the differences in PC composition. Representative image from a single mouse per group is shown in Fig. 2A, B, which resembled the remaining two mice. And, we have arranged ion images of PCs with identical FA compositions at the sn-1 position horizontally, while those with identical FA compositions at the sn-2 position are arranged vertically (Fig. 2A, B).

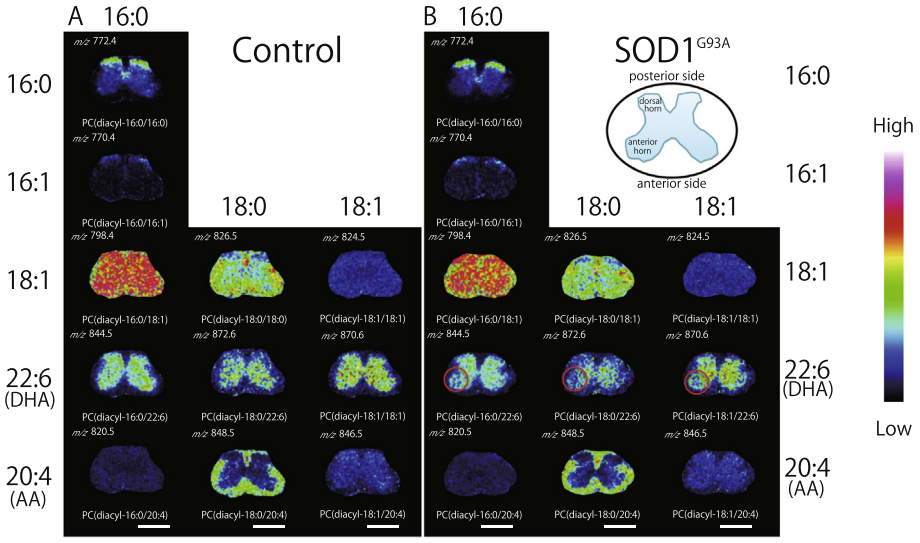

Fig. 2. Distributions of PC species in L5 spinal cords of 22-week-old SOD1^{G93A} and control mice. Ion images of PCs obtained by MALDI-IMS are shown according to their FA compositions. PCs with identical FA compositions at the sn-1 position are arranged horizontally, while those with identical FA compositions at the sn-2 position are arranged vertically. Several specific localizations of PCs were found depending on FA compositions. PCs containing PUFA such as AA (20:4) and DHA (22:6) showed characteristic patterns. Three DHA-containing PCs [PC (16:0/22:6), PC (18:0/22:6), and PC (18:1/22:6)] were abundant in the gray matter in SOD1^{G93A} mice and controls. By contrast, these PCs were reduced in the anterior horn in SOD1^{G93A} compared to control (3A, B red circle). Scale bar = 500 μm. For both control and SOD1^{G93A} mouse, n = 3. (For interpretation of the references to color in this figure legend, the reader is referred to the web version of this article.)

The most abundant PC species, PC (diacyl-16:0/18:1), was uniformly distributed over the entire gray matter region in the control mouse spinal cord (Fig. 2A). In particular, polyunsaturated fatty acids (PUFA), including FA 22:6 [docosahexaenoic acid (DHA)]-containing PCs, showed a selective distribution pattern in gray matter. Three DHA-containing PCs, PC (diacyl-16:0/22:6), PC (diacyl-18:0/22:6), and PC (diacyl-18:1/22:6), were relatively abundant in the gray matter in both control and SOD1^{G93A} spinal cord sections (Fig. 2A, B). Expression of these DHA-containing PCs was reduced in the anterior horn in SOD1^{G93A} (Fig. 2B red circle), whereas expression of the FA 20:4 [arachidonic acid (AA)]-containing PCs, PC (diacyl-16:0/20:4), and PC (diacyl-18:0/20:4) showed no apparent differences between control and SOD1^{G93A} mice (Fig. 2A, B). PC (diacyl-16:0/16:0) was observed specifically in the dorsal horn gray matter, and expression was similar between control and SOD1^{G93A} mice (Fig. 2A, B).

PC (diacyl-16:0/22:6) expression was decreased in the L5 anterior horns of SOD1^{G93A} mice in the terminal stage

To determine when the reduction of PC (diacyl-16:0/22:6) level in the anterior horn begins, the same analysis was performed on sections obtained at different stages of the disease. Analysis using MALDI-IMS showed no significant reductions of PC (diacyl-16:0/22:6) expression in the anterior horn in the pre-symptomatic stage (5-week-old) (Fig. 3A, D) and early disease stage (10-week-old) (Fig. 3B, E). However, we continued to observe a remarkable decrease in the terminal stage (22-week-old) (Fig. 3C, F). Next we semi-quantitatively determined the mean signal intensities of PC (diacyl-16:0/22:6) in the anterior horn in L5 spinal cord sections obtained from both groups at different disease stages using the MALDI-IMS in the positive ion detection mode (n = 3 for each case). We observed that the mean signal intensities corresponding to PC (diacyl-16:0/22:6) in the anterior horn of 22-week-old SOD1^{G93A} mice were significantly lower than those in the age-matched control group (Fig. 3G). We also semi-quantitatively compared the mean signal intensities of PC (diacyl-18:0/22:6) and PC (diacyl-18:1/22:6) in the anterior horn using L5 spinal cord sections similarly obtained from both groups (n = 3 for each group) (Fig. 3H, I). Although non-significant, the mean signal intensities of these two PCs in the anterior horn tended to be lower in the SOD1^{G93A} mice than in control mice. (Fig. 3H, I).

Reductions in PC (diacyl-16:0/22:6) were associated with neuronal loss

To examine reductions in PC (diacyl-16:0/22:6) at the cellular level, we immunostained spinal cord sections of 22-week-old SOD1^{G93A} mice using different cell type-specific markers. While PC (diacyl-16:0/22:6) and NeuN reactivity levels were preserved in the control (Fig. 4A–D) at this age, SOD1^{G93A} mice exhibited a reduction of both PC (diacyl-16:0/22:6) and NeuN reactivity in the anterior horn (Fig. 4E–H). Progressive motor neuron cell death is a characteristic of ALS. Motor neuron expression Hb9 was quantified in 5 (pre-symptomatic stage) (Fig. 4I, L), 10 (early disease stage) (Fig. 4J, M), and 22-week-old mice (terminal stage) (Fig. 4K, N). Large lumbar motor neurons with a cell body area of $\geqslant$450 μm^2 were identified and included using Hb9, specific markers for motor neurons. Thus,

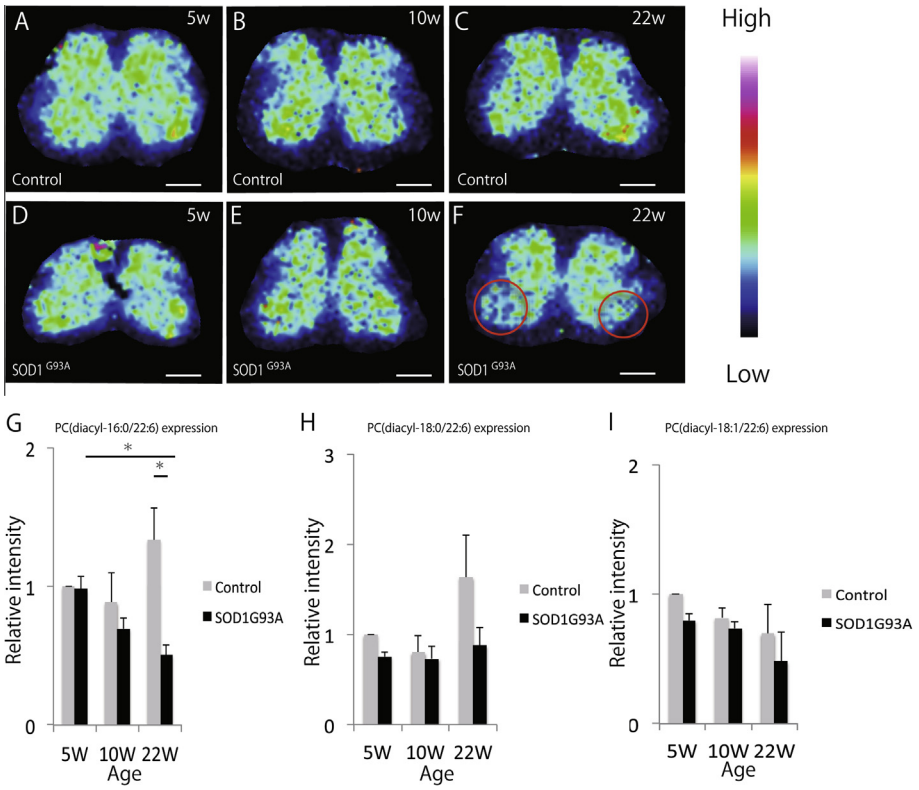

Fig. 3. PC (diacyl-16:0/22:6) expression was decreased in the L5 anterior horns of 22-week-old SOD1^{G93A} mouse. In order to evaluate when the PC (diacyl-16:0/22:6) expression level was decreased, the same analysis was performed at different stages. 5 weeks old is the pre-symptomatic stage (A, D), 10 weeks old is the early stage after disease onset (B, E) and 22 weeks old is the terminal stage (C, F). There were no significant differences observed at the pre-symptomatic stage (A, D) or the early stage after disease onset (B, E). However PC (diacyl-16:0/22:6) expression in SOD1^{G93A} was significantly lower than control at the terminal stage (C, F red circle). Next we compared the mean signal intensities of PC (diacyl-16:0/22:6), PC (diacyl-18:0/22:6) and PC (diacyl-18:1/22:6) in the anterior horn of L5 spinal cord sections obtained from both control and SOD1^{G93A} at week 5, week 10, and week 22 after birth by using MALDI-IMS in the positive ion detection mode (G–I, $n = 3$ for every data point). We observed that the mean signal intensities corresponding to PC (diacyl-16:0/22:6) in the anterior horn in the 22-week-old SOD1^{G93A} mouse group were significantly lower than those in the 22-week-old control group (G). We also semi-quantitatively compared the mean signal intensities of PC (diacyl-18:0/22:6) and PC (diacyl-18:1/22:6) in the anterior horn of L5 spinal cord sections similarly obtained from both groups ($n = 3$ for each group) (H, I). Although non-significant, the mean signal intensities of these two PCs in the anterior horn tended to be lower in SOD1^{G93A} mice than in control mice. (H, I). Scale bar = 200 μm. Error bar represent SEM. Significant differences were confirmed using the criterion of $p < 0.05$ by an unpaired two-sample *t*-test or a one-way ANOVA test. Post-ANOVA comparisons were made using the Tukey test. (For interpretation of the references to color in this figure legend, the reader is referred to the web version of this article.)

only the large α-motor neurons most vulnerable to cell death in ALS were quantified as performed previously (Seijffers et al., 2014). In control mice, no motor neuron cell death was observed at all the stages. On the other hand, we observed a remarkable loss in the number of motor neurons at the terminal stage of SOD1^{G93A} mice (Fig. 4L–O). There was no significant difference in the number of motor neurons in L5 anterior horn between both groups at pre-symptomatic and early disease stages (Fig. 4I-J, L-M).

PC (diacyl-16:0/16:0) expression was preserved in the L5 dorsal horns of SOD1^{G93A} mice in the terminal stage

In evaluating alterations in the levels of PCs in the dorsal horn, we focused on PC (diacyl-16:0/16:0) expression, which was specifically distributed in the dorsal horn. Analysis using MALDI-IMS showed no significant reduction of PC (diacyl-16:0/16:0) expression in the dorsal horn in the pre-symptomatic stage (5-week-old) (Fig. 5A, D), the early stage after disease onset (10-week-old) (Fig. 5B, E), and the terminal stage (22-week-old) (Fig. 5C, F). Next, we semi-quantitatively compared the mean signal intensities of PC (diacyl-16:0/16:0) in dorsal horn L5 spinal cord sections obtained from both groups at the three time points of the disease using MALDI-IMS in the positive ion detection mode ($n = 3$ for each case). We observed no significant differences in the mean signal intensities corresponding to PC (diacyl-16:0/16:0) in the dorsal horn between groups at all stages (Fig. 5G).

DISCUSSION

In this study, we performed MALDI-IMS on lumbar spinal cord tissue sections from SOD1^{G93A} ALS model mice to identify PC species that exhibited significant changes associated with ALS in the presymptomatic, early stage after disease onset, and terminal stages. IMS analysis of spinal cords showed that average spectra detected in the mass range of $700 < m/z < 880$ were almost same

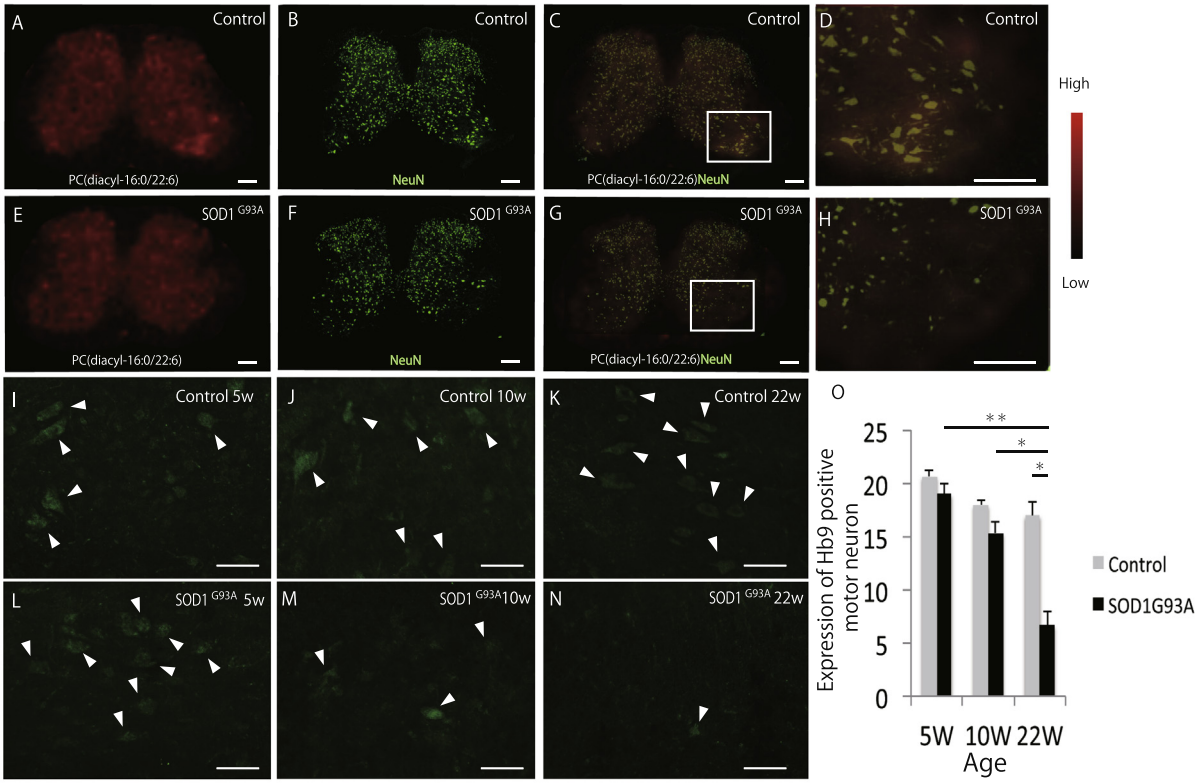

Fig. 4. Reduced PC (diacyl-16:0/22:6) levels were associated with a reduction of NeuN-positive cells in the L5 spinal cord of 22-week-old SOD1^{G93A} mice. Upper figures correspond to control (A–D), and lower figures correspond to SOD1^{G93A} (E–H). A and E show the distribution of PC (diacyl-16:0/22:6). B and F show the NeuN-staining results. C and G show representative merged images showing the PC (diacyl-16:0/22:6) distribution and NeuN-staining. D and H show magnified images of the boxed area in C and G. A reduction of PC (diacyl-16:0/22:6) was found in the site where NeuN-positive neurons have been lost. I–N show the Hb9-staining results. Large lumbar motor neurons with a cell body area of $\geqslant$450 μm^2 were identified and stained using Hb9, specific markers for motor neurons. In control mice, no motor neuron cell death was observed at any stage. On the other hand, we observed a remarkable loss in the number of motor neuron at the terminal stage in SOD1^{G93A} mice (L–O). There was no significant difference in the number of motor neurons in L5 anterior horn between both groups at pre-symptomatic and early disease stages (I-J, L-M). Error bars represent SEMs. Significant differences were confirmed using the criterion of $p < 0.05$ by an unpaired two-sample *t*-test or a one-way ANOVA test. Post-ANOVA comparisons were made using Tukey's test. A–H; Scale bar = 100 μm. I–N; Scale bar = 50 μm. $^{*}p < 0.05$, $^{**}p < 0.01$.

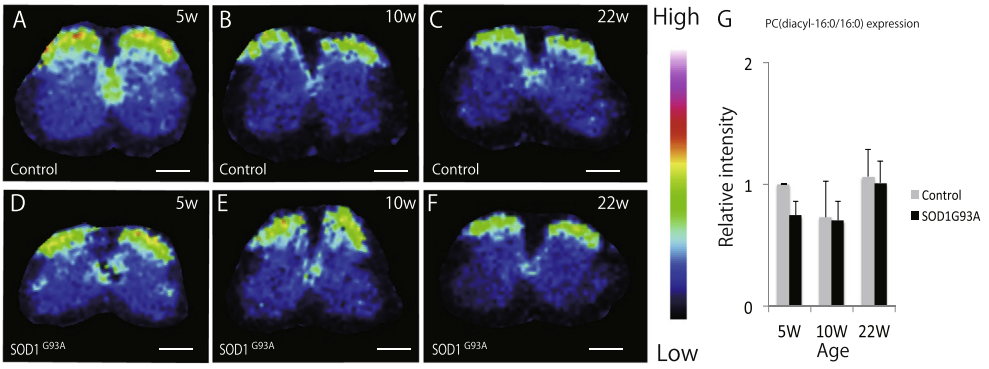

Fig. 5. PC (diacyl-16:0/16:0) expression was preserved in the L5 dorsal horns of 22 week-old SOD1^{G93A} mouse. Analysis using MALDI-IMS showed no significant reduction of PC (diacyl-16:0/16:0) expression in the dorsal horn in the pre-symptomatic stage (5-week old) (A, D), the early stage after disease onset (10-week old) (B, E), and the terminal stage (22-week old) (C, F). Next we compared the mean signal intensities of PC (diacyl-16:0/16:0) in the dorsal horn of L5 spinal cord sections obtained from both control and SOD1^{G93A} at 5, 10, and 22 weeks after birth using MALDI-IMS in the positive ion detection mode (G, $n = 3$ for every case). There were no significant differences observed in the mean signal intensities corresponding to PC (diacyl-16:0/16:0) in the anterior horn between both groups at all stages (G). Scale bar = 200 μm. Error bars represent SEMs. Significant differences were confirmed using the criterion of $p < 0.05$ by an unpaired two-sample *t*-test or a one-way ANOVA test.

between ALS mice and control in the terminal stage (22 weeks) (Fig. 1A, B). Among the observed peaks, 12 were determined to be PC molecular species and were visualized using special software, flexImaging 2.0 (Fig. 2A, B). Since we used a matrix with potassium acetate for the PC evaluation, all the PC molecular

species can be considered to be K^+ adducts. It was previously reported that PC molecular species observed at *m/z* 772.4, PC (diacyl-16:0/16:0, K^+ adduct), are localized in the gray matter region, especially in the dorsal horn (Landgraf et al., 2009; Hanada et al., 2012; Sugiura et al., 2012). We found that the expression of PC (diacyl-16:0/16:0) in the dorsal horn of $SOD1^{G93A}$ ALS model mice was preserved in the terminal stage (Fig. 5). The dorsal horn is mainly comprised of secondary sensory neurons. Therefore, our observation that PC (diacyl-16:0/16:0) was preserved in this region even at the terminal stage may indicate that sensory functions of ALS patients are largely preserved until extremely late stages of the disease.

In contrast, we found that expression of PC (diacyl-16:0/22:6), PC (diacyl-18:0/22:6), and PC (diacyl-18:1/22:6) was lower in the anterior horn of ALS mice at terminal stages compared to age matched controls (Fig. 2A, B). Interestingly, these PCs are DHA-containing and reductions of DHA have been observed in the spinal cord of ALS patients (Ilieva et al., 2007).

DHA is a major component of neural membrane phospholipids and has potential role related to memory, learning, and cognitive processes. Previous reports also show that administration of DHA leads to an improvement of learning ability. Additionally, DHA is involved in signal transduction, neuronal differentiation, neurogenesis, and protection against synaptic loss or spinal cord injury (Arima et al., 2014). These findings thus imply that DHA-containing PCs play important roles in the development, normal physiology, and degeneration of the nervous system. In a previous report, reduction of DHA-containing PCs was markedly decreased in the gray matter of human Alzheimer's disease brains, which was significantly correlated with disease duration (Yuki et al., 2014). Furthermore, at the molecular level, this depletion was associated with reduced levels of the postsynaptic protein PSD-95 but not the presynaptic protein synaptophysin. Interestingly, this reduction in PC (diacyl-18:0/22:6) levels did not correlate with the degrees of Aβ deposition and neuronal loss in Alzheimer's disease (Yuki et al., 2014). In the anterior horn of our $SOD1^{G93A}$ ALS model mice, we observed alterations of PC (diacyl-16:0/22:6), which is also a DHA-containing PCs, in the terminal, but not earlier disease stage (Fig. 3). Alterations of DHA-containing PCs were not found in other gray or white matter regions including the anterior, lateral, and posterior funiculus. We further confirmed that the reduction of DHA-containing PCs and of Hb9-positive motor neurons in the anterior horn occurred simultaneously in the ALS terminal stage and they seemed to be colocalized spatiotemporarily (Figs. 3 and 4). Thus, the reduction of DHA could be reflecting the loss (apoptosis) of motor neurons themselves in the anterior horn of the spinal cord in ALS mice. In addition, the reduction of DHA could be affecting on the motor endplate, leading to the ''dying back'' of the motor axons from the neuromuscular junction.

As DHA contains six double bonds, it is likely to be oxidized by free radicals (Schafer et al., 2000; Yuki et al., 2014). Indeed, a biochemical study has demonstrated that lipid peroxidation was enhanced in spinal cord motor neurons of ALS patients (Shibata et al., 2001). Therefore, the cause of the compositional decrease of DHA-containing PCs in the anterior horn of ALS mouse might be oxidative stress.

Our findings suggest that reductions of DHA levels might be important in ALS, while other work suggests that dietary intake of DHA is effective in regulating brain DHA levels. Rodent studies have revealed that levels of DHA-containing phospholipids in the central nervous system are decreased by depletions of DHA in the diet (Garcia et al., 1998; Hamilton et al., 2000). Oral supplementation with DHA has been shown to elevate brain DHA levels in rats (Hashimoto et al., 2002). There are several reports that omega-3 FA (e.g., DHA) treatment has neuroprotective effects against central nervous system injury and aging (King et al., 2006; Dyall et al., 2010; Lim et al., 2010). However, the mechanisms underlying these therapeutic effects are still poorly understood.

In contrast, it was reported that dietary supplementation with eicosapentaenoic acid (20:5, EPA), which is converted to DHA *in vivo*, increased the numbers of activated microglia and astrocytes in the brain of an ALS mouse model (Yip et al., 2013). Moreover, treatment with EPA initiated at the pre-symptomatic stage led to a significantly shorter lifespan (Yip et al., 2013). The authors thus concluded that dietary EPA supplementation in ALS patients was not effective, but rather harmful. Taking these findings into consideration, the decrease of DHA-containing PCs in the anterior horn of ALS mice observed in this study was unlikely to be a cause of disease progression, but rather may have been a reflection of it.

In the future, we must clarify the cause of the decrease of DHA-containing PCs in the anterior horn of ALS model mice and the role of DHA-containing PCs in neuronal cells in more detail. Further elucidating the characteristics and biological roles of DHA containing PCs in ALS is expected to be useful in the prevention of ALS and the development of therapeutic agents for ALS. Moreover, pathological studies have shown that the cranial motor nuclei of the oculomotor, trochlear, and abducens nerves, and Onuf's nucleus in the sacral spinal cord are relatively spared in human ALS (Mannen et al., 1977; Okamoto et al., 1993; Brockington et al., 2013). Therefore, analysis of such DHA-containing lipids in these neurons and their comparison with those in the anterior horn of spinal cord at the level of L5 can provide valuable insights about pathology of this disease.

CONCLUSION

Our data revealed a significant decrease in DHA-containing PCs in the anterior horn of the spinal cord of ALS mice in the terminal stage, which may reflect neuronal loss. These findings indicate that ALS spinal cords may show significant alterations in PC metabolism present only in the terminal stage of the disease.

CONFLICT OF INTEREST

The authors declare no conflict of interest.

CONTRIBUTORS

H.A., M.H., and T.O. designed the study, directed all experiments, and wrote the manuscript. K.K., H.T., and K.K. provided animals and supervised the animal experiments H.A. and D.X. acquired the data for this study. H.A., T.O., T.H., N.M., M.H., and M.S. performed the data analysis, and H.A., T.O., T.H., N.M., and M.H. H.A., T.O., T.H., N.M., M.H., K.K., T.H., K.K., Y.M., and M.S. contributed to data interpretation. All authors read and approved the final manuscript.

Acknowledgments—This work was supported by JSPS–JAPAN KAKENHI Grant Numbers 25116712 for M.S. and 24592192 for Y.M. We would like to thank Ms. Ayako Okamoto for her excellent technical assistance.

REFERENCES

Acquadro E, Caron I, Tortarolo M, Bucci EM, Bendotti C, Corpillo D (2014) Human SOD1-G93A specific distribution evidenced in murine brain of a transgenic model for amyotrophic lateral sclerosis by MALDI imaging mass spectrometry. J Proteome Res 13:1800–1809.

Arima H, Hanada M, Hayasaka T, Masaki N, Omura T, Xu D, Hasegawa T, Togawa D, Yamato Y, Kobayashi S, Yasuda T, Matsuyama Y, Setou M (2014) Blockade of IL-6 signaling by MR16-1 inhibits reduction of docosahexaenoic acid-containing phosphatidylcholine levels in a mouse model of spinal cord injury. Neuroscience 269:1–10.

Bendotti C, Carri MT (2004) Lessons from models of SOD1-linked familial ALS. Trends Mol Med 10:393–400.

Brockington A, Ning K, Heath PR, Wood E, Kirby J, Fusi N, Lawrence N, Wharton SB, Ince PG, Shaw PJ (2013) Unravelling the enigma of selective vulnerability in neurodegeneration: motor neurons resistant to degeneration in ALS show distinct gene expression characteristics and decreased susceptibility to excitotoxicity. Acta Neuropathol 125:95–109.

Bruijn LI, Houseweart MK, Kato S, Anderson KL, Anderson SD, Ohama E, Reaume AG, Scott RW, Cleveland DW (1998) Aggregation and motor neuron toxicity of an ALS-linked SOD1 mutant independent from wild-type SOD1. Science 281:1851–1854.

Clement AM, Nguyen MD, Roberts EA, Garcia ML, Boillee S, Rule M, McMahon AP, Doucette W, Siwek D, Ferrante RJ, Brown Jr RH, Julien JP, Goldstein LS, Cleveland DW (2003) Wild-type nonneuronal cells extend survival of SOD1 mutant motor neurons in ALS mice. Science 302:113–117.

Di Giorgio FP, Carrasco MA, Siao MC, Maniatis T, Eggan K (2007) Non-cell autonomous effect of glia on motor neurons in an embryonic stem cell-based ALS model. Nat Neurosci 10:608–614.

Dyall SC, Michael GJ, Michael-Titus AT (2010) Omega-3 fatty acids reverse age-related decreases in nuclear receptors and increase neurogenesis in old rats. J Neurosci Res 88:2091–2102.

Garcia MC, Ward G, Ma YC, Salem Jr N, Kim HY (1998) Effect of docosahexaenoic acid on the synthesis of phosphatidylserine in rat brain in microsomes and C6 glioma cells. J Neurochem 70:24–30.

Gurney ME, Pu H, Chiu AY, Dal Canto MC, Polchow CY, Alexander DD, Caliendo J, Hentati A, Kwon YW, Deng HX, et al. (1994) Motor neuron degeneration in mice that express a human Cu, Zn superoxide dismutase mutation. Science 264:1772–1775.

Hamilton L, Greiner R, Salem Jr N, Kim HY (2000) N-3 fatty acid deficiency decreases phosphatidylserine accumulation selectively in neuronal tissues. Lipids 35:863–869.

Hanada M, Sugiura Y, Shinjo R, Masaki N, Imagama S, Ishiguro N, Matsuyama Y, Setou M (2012) Spatiotemporal alteration of phospholipids and prostaglandins in a rat model of spinal cord injury. Anal Bioanal Chem 403:1873–1884.

Hanrieder J, Ekegren T, Andersson M, Bergquist J (2013) MALDI imaging of post-mortem human spinal cord in amyotrophic lateral sclerosis. J Neurochem 124:695–707.

Hashimoto M, Hossain S, Shimada T, Sugioka K, Yamasaki H, Fujii Y, Ishibashi Y, Oka J, Shido O (2002) Docosahexaenoic acid provides protection from impairment of learning ability in Alzheimer's disease model rats. J Neurochem 81:1084–1091.

Hayasaka T, Goto-Inoue N, Sugiura Y, Zaima N, Nakanishi H, Ohishi K, Nakanishi S, Naito T, Taguchi R, Setou M (2008) Matrix-assisted laser desorption/ionization quadrupole ion trap time-of-flight (MALDI-QIT-TOF)-based imaging mass spectrometry reveals a layered distribution of phospholipid molecular species in the mouse retina. Rapid Commun Mass Spectrom 22:3415–3426.

Hayworth CR, Gonzalez-Lima F (2009) Pre-symptomatic detection of chronic motor deficits and genotype prediction in congenic B6.SOD1(G93A) ALS mouse model. Neuroscience 164:975–985.

Hirano K, Ohgomori T, Kobayashi K, Tanaka F, Matsumoto T, Natori T, Matsuyama Y, Uchimura K, Sakamoto K, Takeuchi H, Hirakawa A, Suzumura A, Sobue G, Ishiguro N, Imagama S, Kadomatsu K (2013) Ablation of keratan sulfate accelerates early phase pathogenesis of ALS. PLoS One 8:e66969.

Ilieva EV, Ayala V, Jove M, Dalfo E, Cacabelos D, Povedano M, Bellmunt MJ, Ferrer I, Pamplona R, Portero-Otin M (2007) Oxidative and endoplasmic reticulum stress interplay in sporadic amyotrophic lateral sclerosis. Brain 130:3111–3123.

Jackson SN, Ugarov M, Egan T, Post JD, Langlais D, Albert Schultz J, Woods AS (2007) MALDI-ion mobility-TOFMS imaging of lipids in rat brain tissue. J Mass Spectrom 42:1093–1098.

Jackson SN, Wang HY, Woods AS (2005) *In situ* structural characterization of phosphatidylcholines in brain tissue using MALDI-MS/MS. J Am Soc Mass Spectrom 16:2052–2056.

King VR, Huang WL, Dyall SC, Curran OE, Priestley JV, Michael-Titus AT (2006) Omega-3 fatty acids improve recovery, whereas omega-6 fatty acids worsen outcome, after spinal cord injury in the adult rat. J Neurosci 26:4672–4680.

Kobayashi K, Imagama S, Ohgomori T, Hirano K, Uchimura K, Sakamoto K, Hirakawa A, Takeuchi H, Suzumura A, Ishiguro N, Kadomatsu K (2013) Minocycline selectively inhibits M1 polarization of microglia. Cell Death Dis 4:e525.

Landgraf RR, Prieto Conaway MC, Garrett TJ, Stacpoole PW, Yost RA (2009) Imaging of lipids in spinal cord using intermediate pressure matrix-assisted laser desorption-linear ion trap/Orbitrap MS. Anal Chem 81:8488–8495.

Lim SN, Huang W, Hall JC, Ward RE, Priestley JV, Michael-Titus AT (2010) The acute administration of eicosapentaenoic acid is neuroprotective after spinal cord compression injury in rats. Prostaglandins Leukot Essent Fatty Acids 83:193–201.

Mannen T, Iwata M, Toyokura Y, Nagashima K (1977) Preservation of a certain motoneurone group of the sacral cord in amyotrophic lateral sclerosis: its clinical significance. J Neurol Neurosurg Psychiatry 40:464–469.

McLean JA, Ridenour WB, Caprioli RM (2007) Profiling and imaging of tissues by imaging ion mobility-mass spectrometry. J Mass Spectrom 42:1099–1105.

Okamoto K, Hirai S, Amari M, Iizuka T, Watanabe M, Murakami N, Takatama M (1993) Oculomotor nuclear pathology in amyotrophic lateral sclerosis. Acta Neuropathol 85:458–462.

Piomelli D, Astarita G, Rapaka R (2007) A neuroscientist's guide to lipidomics. Nat Rev Neurosci 8:743–754.

Rosen DR, Siddique T, Patterson D, Figlewicz DA, Sapp P, Hentati A, Donaldson D, Goto J, O'Regan JP, Deng HX, et al. (1993) Mutations in Cu/Zn superoxide dismutase gene are associated with familial amyotrophic lateral sclerosis. Nature 362:59–62.

Schafer FQ, Qian SY, Buettner GR (2000) Iron and free radical oxidations in cell membranes. Cell Mol Biol 46:657–662.

Shibata N, Nagai R, Uchida K, Horiuchi S, Yamada S, Hirano A, Kawaguchi M, Yamamoto T, Sasaki S, Kobayashi M (2001) Morphological evidence for lipid peroxidation and protein

glycoxidation in spinal cords from sporadic amyotrophic lateral sclerosis patients. Brain Res 917:97–104.

Sugiura Y, Konishi Y, Zaima N, Kajihara S, Nakanishi H, Taguchi R, Setou M (2009) Visualization of the cell-selective distribution of PUFA-containing phosphatidylcholines in mouse brain by imaging mass spectrometry. J Lipid Res 50:1776–1788.

Sugiura Y, Setou M (2010) Imaging mass spectrometry for visualization of drug and endogenous metabolite distribution: toward *in situ* pharmacometabolomes. J Neuroimmune Pharmacol 5:31–43.

Sugiura Y, Zaima N, Setou M, Ito S, Yao I (2012) Visualization of acetylcholine distribution in central nervous system tissue sections by tandem imaging mass spectrometry. Anal Bioanal Chem 403:1851–1861.

Takeuchi H, Mizoguchi H, Doi Y, Jin S, Noda M, Liang J, Li H, Zhou Y, Mori R, Yasuoka S, Li E, Parajuli B, Kawanokuchi J, Sonobe Y, Sato J, Yamanaka K, Sobue G, Mizuno T, Suzumura A (2011) Blockade of gap junction hemichannel suppresses disease progression in mouse models of amyotrophic lateral sclerosis and Alzheimer's disease. PLoS one 6:e21108.

van Meer G, Voelker DR, Feigenson GW (2008) Membrane lipids: where they are and how they behave. Nat Rev Mol Cell Biol 9:112–124.

Wisztorski M, Croix D, Macagno E, Fournier I, Salzet M (2008) Molecular MALDI imaging: an emerging technology for neuroscience studies. Dev Neurobiol 68:845–858.

Yip PK, Pizzasegola C, Gladman S, Biggio ML, Marino M, Jayasinghe M, Ullah F, Dyall SC, Malaspina A, Bendotti C, Michael-Titus A (2013) The omega-3 fatty acid eicosapentaenoic acid accelerates disease progression in a model of amyotrophic lateral sclerosis. PLoS One 8:e61626.

Yuki D, Sugiura Y, Zaima N, Akatsu H, Takei S, Yao I, Maesako M, Kinoshita A, Yamamoto T, Kon R, Sugiyama K, Setou M (2014) DHA-PC and PSD-95 decrease after loss of synaptophysin and before neuronal loss in patients with Alzheimer's disease. Sci Rep 4:7130.

(Accepted 25 March 2015)
(Available online 2 April 2015)